*Progress In Electromagnetics Research C, Vol. 41, 27–39, 2013*

# ULTRA-WIDEBAND MULTI-STUB LOADED RING RESONATOR BANDPASS FILTER WITH A NOTCHED-BAND

**Zhi-Peng Li*, Tao Su, Yong-Liang Zhang, Sheng-Jie Wang, and Chang-Hong Liang**

National Laboratory of Science and Technology on Antennas and Microwaves, Xidian University, Xi'an, Shaanxi 710071, People's Republic of China

**Abstract**—In this paper, a novel compact ultra-wideband (UWB) microstrip bandpass filter (BPF) with a notched band using the proposed multi-stub loaded ring resonator (MSLRR) is presented. The MSLRR is constructed by loading four open stubs in a ring resonator, i.e., one pair of high-impedance stub at the top side and another two low-impedance stubs at the bottom side locations. Five modes, including two odd modes and three even modes, could be designed within UWB band. Moreover, two transmission zeros (TZs) are generated by the ring structure, leading to a quasi-elliptic function response that enhances the selectivity significantly. Two slotline split-ring resonators (SRR) are used to create a narrow notched band at 8.6 GHz. The simulated and measured results are in good agreement and show good in-band filtering performance and sharp selectivity.

## 1. INTRODUCTION

Since the release of ultra-wideband (UWB) frequency spectrum (range of 3.1–10.6 GHz) for commercial communication application in 2002 [1], more attention has been paid to applications of UWB technology on wireless communication system. The UWB bandpass filter is one of the key passive components in a UWB radio communication system. Hence, various UWB BPFs have been proposed via different methods and structures [2–10]. In [2], a UWB bandpass filter was proposed using a combination of lowpass and highpass filters (HPF), which

*Received 15 May 2013, Accepted 9 June 2013, Scheduled 12 June 2013*

* Corresponding author: Zhi-Peng Li (shengjie8411@163.com).

is convenient to design. However, the physical size of this filter is relatively large. In order to have smaller circuit size, multi-mode resonator (MMR) is introduced [3–8]. The first several resonant frequencies of MMR were properly adjusted to be placed quasi equally within the UWB. With the development of wireless communication technology, UWB bandpass filters with good in-band transmission characteristics and sharp selectivity are highly demanded. In [9, 10], stub loaded resonators (SLR) were used, which had multiple-mode resonant characteristic and two tunable transmission zeros (TZs). Cross coupling between nonadjacent resonators or source and load has also been widely used to design ultra-wideband BPFs [11, 12]. In [13], a novel modified composite right/left-handed (CRLH) resonators were used to achieve a UWB BPF. Furthermore, the UWB frequency band may be interfered by the satellite-communication signal. Thus, a narrow-band notched UWB BPF needs to be developed. Thus, many notched-band designing technologies, such as asymmetric interdigital coupled feed line [14], defected split-ring resonator [15], semi-complementary split ring resonator [16], have been reported. In addition, multiple notch-band UWB BPFs is the trend of future development [17–22].

Recently, the ring resonators are utilized to explore bandpass filters with a wide fractional passband [23, 24]. In this paper, a novel compact UWB BPF with notched band and sharp skirt for the use in wireless systems is proposed. A UWB BPF is built up by the multi-stub loaded ring resonator, which has an excellent in-band performance and allows controlling the resonant frequencies sensitively. In order to

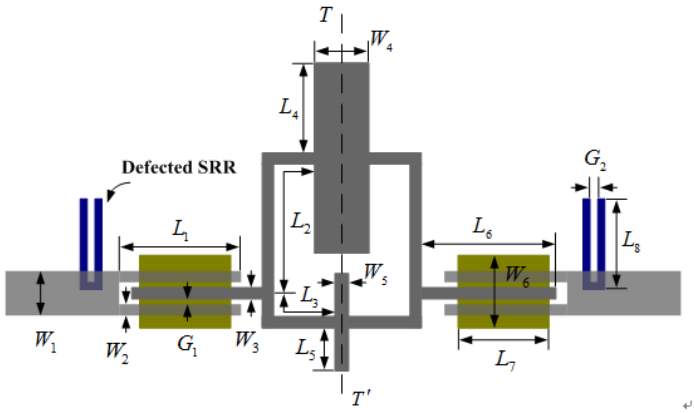


**Figure 1.** Proposed UWB BPF.

get notched band, SRR are embedded in the I/O line without enlarging the size of the filter. The center and bandwidth of the notched band can be controlled by adjusting the length and gap of the stubs. A compact planar UWB BPF using the presented multi-stub loaded ring resonator, as shown in Figure 1, is designed, fabricated and measured for validation and the simulations and measurements agree well with each other.

## 2. MULTI-STUB LOADED RING RESONATOR

Figure 2(a) is the basic structure of the proposed multi-stub loaded ring resonator. It is a conventional ring resonator with four stubs. The ring resonator with impedance $Z_1$ and electrical length $\theta_1$, $\theta_2$ and $\theta_3$ is in the primary position, while four open stubs are vertically loaded, i.e., two open stubs of impedance $Z_2$, electrical length $\theta_4$ at the top side and another two open stubs of impedance $Z_3$, electrical length $\theta_5$ at the bottom side.

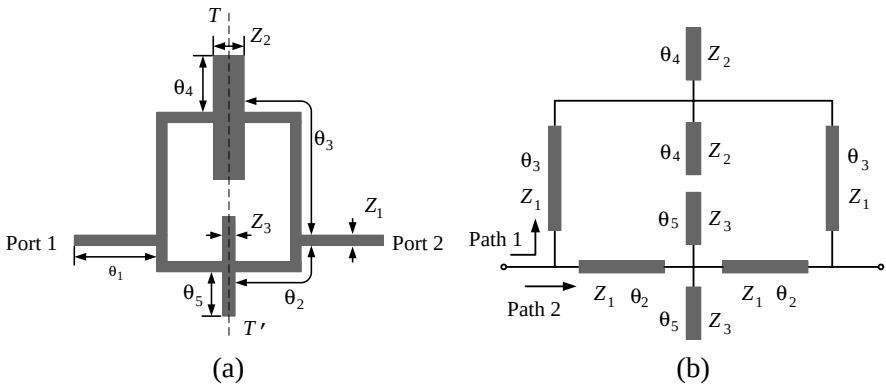


**Figure 2.** (a) The multi-stub loaded ring resonant. (b) Schematics of a MSLRR.

As studied in [25], for a ring resonator band-pass filter, two TZs are produced in the lower and upper cutoff edges of the desired pass band resulting from electric currents in the two propagation paths (Path 1 and Path 2) canceling each other. Two transmission zeros of the ring in the proposed resonator decide the bandwidth of the filter. Its equivalent circuit is shown in Figure 2(b). Based on the transmission line theory, The $ABCD$-matrices of the open stubs, transmission lines

are [26]:

$$M_{line\_t}=\begin{bmatrix}\cos\theta_3 & jZ_1\sin\theta_3\\ j\sin\theta_3/Z_1 & \cos\theta_3\end{bmatrix},\quad M_{stub\_t}=\begin{bmatrix}1 & 0\\ j\tan\theta_4/Z_2 & 1\end{bmatrix} \tag{1a}$$

$$M_{line\_b}=\begin{bmatrix}\cos\theta_2 & jZ_1\sin\theta_2\\ j\sin\theta_2/Z_1 & \cos\theta_2\end{bmatrix},\quad M_{stub\_b}=\begin{bmatrix}1 & 0\\ j\tan\theta_5/Z_3 & 1\end{bmatrix} \tag{1b}$$

For Path 1, the $ABCD$-matrix is $M_{line\_t} \times M_{stub\_t} \times M_{stub\_t} \times M_{line\_t}$ ($M_{line\_t}$ — transmission line $\theta_3$, $M_{stub\_t}$ — open stub $\theta_4$). For Path 2, the $ABCD$-matrix is $M_{line\_b} \times M_{stub\_b} \times M_{stub\_b} \times M_{line\_b}$ ($M_{line\_b}$-transmission line $\theta_2$, $M_{stub\_b}$ — open stub $\theta_5$). After the $ABCD$- and $Y$-parameter conversions, the $S$-parameters of the UWB filter can be illustrated as:

$$S_{11}=\frac{Y_0^2-Y_{11}^2+Y_{21}^2}{(Y_0+Y_{11})^2-Y_{21}^2},\quad S_{21}=\frac{-2Y_{21}Y_0}{(Y_0+Y_{11})^2-Y_{21}^2} \tag{2}$$

And $Y_0 = 1/Z_0$ ($Z_0 = 50\,\Omega$). Hence, at the frequencies of transmission zeros, the mutual admittance between the two port must be zero, i.e., $Y_{21} = Y_{12} = 0$. It can be expressed as follow:

$$R_zR_s(\sin 2\theta_2+\sin 2\theta_3)=2R_z\sin^2\theta_2\tan\theta_5+2R_s\sin^2\theta_3\tan\theta_4 \tag{3}$$

where $R_Z = Z_2/Z_1$, $R_S = Z_3/Z_1$.

Based on Formula (3), the dependences of TZs on the normalized stub length $t(=\theta_5/\theta_4)$ and impedance ratios $R_s$ and $R_z$ are shown in Figure 3. Figure 3(a) plots the ratio of the first two transmission zeros frequencies, i.e., $f_{z2}/f_{z1}$, with respect to the length ratio $t$ under

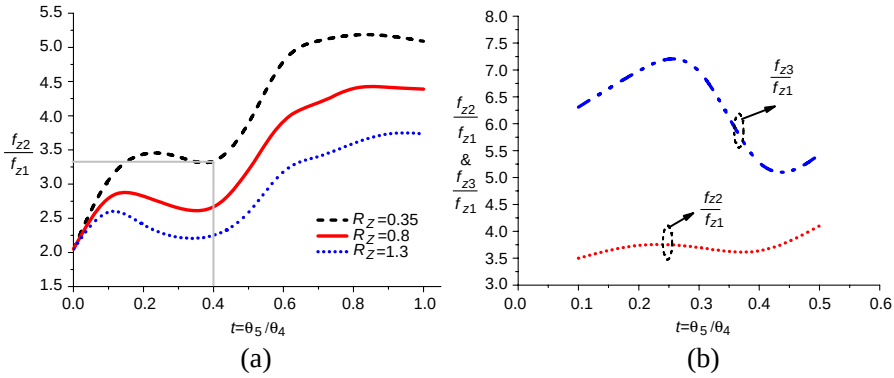


**Figure 3.** (a) Normalized frequencies of transmission zeros ($f_{z2}/f_{z1}$) versus $t$ and $R_z$ ($R_s = 0.9$). (b) Normalized frequencies of transmission zeros ($f_{z2}/f_{z1}f_{z3}/f_{z1}$) versus $t$ ($R_z = 0.35$, $R_s = 0.9$).

$R_s = 0.9$, $R_z = 0.35$, 0.8, 1.3 and $\theta_2 = 2\theta_5$, $\theta_2 + \theta_3 = 6\theta_5$. As $t$ increases from 0 to 1, all lines start with $f_{z2}/f_{z1} \approx 2$ and the tendency of bandwidth between the first and second transmission zeros increases. Furthermore, the bandwidth between the first and second transmission zeros decreases with $R_z$ changing from 0.35 to 1.3. To get an ultra-wideband of 3 dB fractional bandwidth for the final filter, the ratio of the two transmission zeros should be larger than 3.2, and here we choose $f_{z2}/f_{z1} \approx 3.3$, which corresponds that $t \approx 0.4$ and $R_z = 0.35$. Figure 3(b) plots the two normalized transmission zero frequencies, i.e., $f_{z2}/f_{z1}$ and $f_{z3}/f_{z1}$, under $R_z = 0.35$, $R_s = 0.9$. $f_{z3}$ denotes the third transmission zero. It can be found that $f_{z2}/f_{z1} \approx 5.3$ when $t \approx 0.4$. It means that a wide stop-band can be obtained.

To understand the resonant behavior of MSLRR, the analysis of resonant modes is required. With the even- and odd-mode excitations at two ports (shown in Figure 2(a)), the diagonal line can be considered as a perfect magnetic wall and electric wall. As such, two of the half symmetrical line resonators can be formed with ideal open- and short-circuited ends at two sides, as shown in Figures 4(a) and (b), respectively.

In the even-mode case, with ideal open-circuited terminals at four ends in Figure 4(a), the odd-mode input admittance can be derived with the superscript "$e$" as the following:

$$Y^e = Z_L^e + Z_R^e \tag{4}$$

with

$$Z_L^e = -jZ_1 \cot\theta_1 \tag{5a}$$

$$Z_R^e = Z_M^e \cdot Z_N^e / (Z_M^e + Z_N^e) \tag{5b}$$

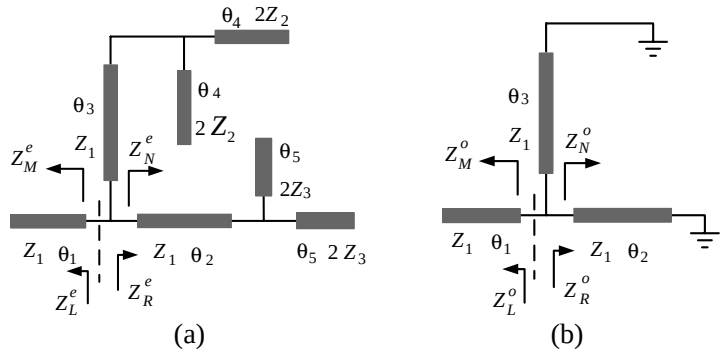


**Figure 4.** (a) and (b) Equivalent even- and odd-mode circuits of a MSLRR, as shown in Figure 2(a).

where

$$Z_M^e = jZ_1(\tan\theta_3 - R_Z\cot\theta_4)/(1 + R_Z\cot\theta_4\tan\theta_3) \quad (6a)$$
$$Z_N^e = jZ_1(\tan\theta_2 - R_S\cot\theta_5)/(1 + R_S\cot\theta_5\tan\theta_2) \quad (6b)$$

If $Y^e = 0$, we can derive the resonance condition to determine the odd-mode resonant frequencies.

Similarly, for the odd-mode case, the input admittance can be expressed with the superscript "$o$" as follows:

$$Y^\circ = Z_L^\circ + Z_R^\circ \quad (7)$$

with

$$Z_L^\circ = -jZ_1\cot\theta_1 \quad (8a)$$
$$Z_R^\circ = Z_M^\circ \cdot Z_N^\circ/(Z_M^\circ + Z_N^\circ) \quad (8b)$$

where

$$Z_M^\circ = jZ_1\tan\theta_3 \quad (9a)$$
$$Z_N^\circ = jZ_1\tan\theta_2 \quad (9b)$$

If $Y^\circ = 0$, the even-mode resonant frequencies can be determined.

Based on the above analysis, resonant frequencies of all the even- and odd-order modes can be solved as roots of $Y^e = 0$ and $Y^\circ = 0$, respectively. In practice, to understand how to shift resonance frequencies of the resonator by changing its relevant structural parameters might be useful to users. Figure 5 plots the first five normalized resonant frequencies $f_{e3}/f'_{o1}$, $f_{o2}/f'_{o1}$, $f_{e2}/f'_{o1}$, $f_{o1}/f'_{o1}$ and $f_{e1}/f'_{o1}$ versus the normalized arm length of $t' = \theta_3/\theta_1$

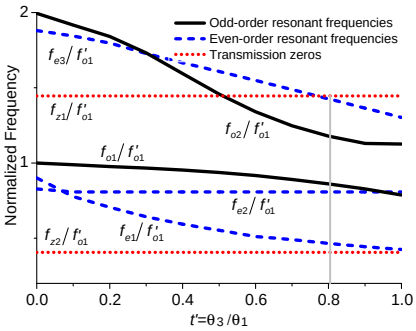


**Figure 5.** Normalized resonator characteristics of the proposed MSLRR versus the normalized arm length of $\theta_3/\theta_1$.

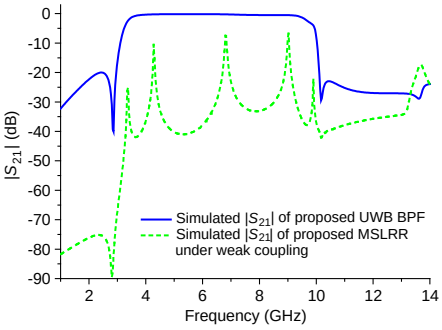


**Figure 6.** Comparison of the simulated $|S_{21}|$ of the proposed UWB BPF.

under the fixed $R_z = 0.35$, $R_s = 0.9$, and $t = \theta_5/\theta_4 = 0.4$, where $f'_{o1}$ is the first odd-mode resonant frequency at $t' = 0$. As can be seen in Figure 5, with $t'$ increasing from 0 to 1.0, these five resonant frequencies seem to be synchronously reduced. Particularly, the third even-mode and second odd-mode resonant frequencies decrease dramatically, thus approaching the frequency range where the other three resonant frequencies are allocated. Besides, the two normalized transmission zeros which are located at the same positions while $t'$ changes. It is implied that, the transmission phases along path 1 and path 2 in the middle of this MSLRR remain unchanged, thus allowing two transmission zeros to remain stationary. When $t' > 0.78$, these normalized resonant frequencies are distributed in the range between the two transmission zeros. At $t' = 0.83$, the five transmission poles are relatively uniformly located in the pass band. Moreover, due to $f_{z1}/f'_{o1}$ and $f_{z2}/f'_{o1}$ are close to $f_{e3}/f'_{o1}$ and $f_{e1}/f'_{o1}$, respectively, at $t' = 0.83$. Thus, good selectivity can be obtained.

The resonant frequencies of proposed MMR under weak coupling are plotted in Figure 6. Five resonant peaks could be obviously observed, and two transmission zeros at the lower and upper cutoff frequencies are introduced by the four center stubs.

## 3. BAND-NOTCHED UWB BPF

As demonstrated in Figure 7(a), in order to introduce a very narrow notched (rejection) band in the UWB passband, two embedded slotline split-ring resonators are arranged in the I/O line, and the whole circuit will not enlarged [16]. The SRR will have an infinite reactance around the desired frequency, which will block the signal at this frequency range transferring from the input port to output port and thus, a notched band is generated. To demonstrate this performance, a single SRR with different lengths and gaps is investigated and its relevant simulated $|S_{21}|$-magnitudes are plotted in Figures 7(b) and 7(c). As the length of $L_8$ varies from 5.5 to 7.5 mm ($G_2$ is fixed at 0.3 mm), the transmission zero gets a gradual increment from 7.1 to 9.6 GHz. With the increased $G_2$ (changing from 0.2 to 0.8 mm), the 3-dB notch bandwidth is decreased. It should be noted that if notch-band moves towards the lower frequency, then the upper stop-band of the filter is reduced by the higher harmonic perturbation.

Based on the above analysis, by applying a strong feed coupling to the presented MSLRR as shown in Figure 1, i.e., the parallel-coupled feed lines with two aperture-backed at the two sides [14], an ultra-wideband BPF is realized. The "S.F." stands for the skirt factor of

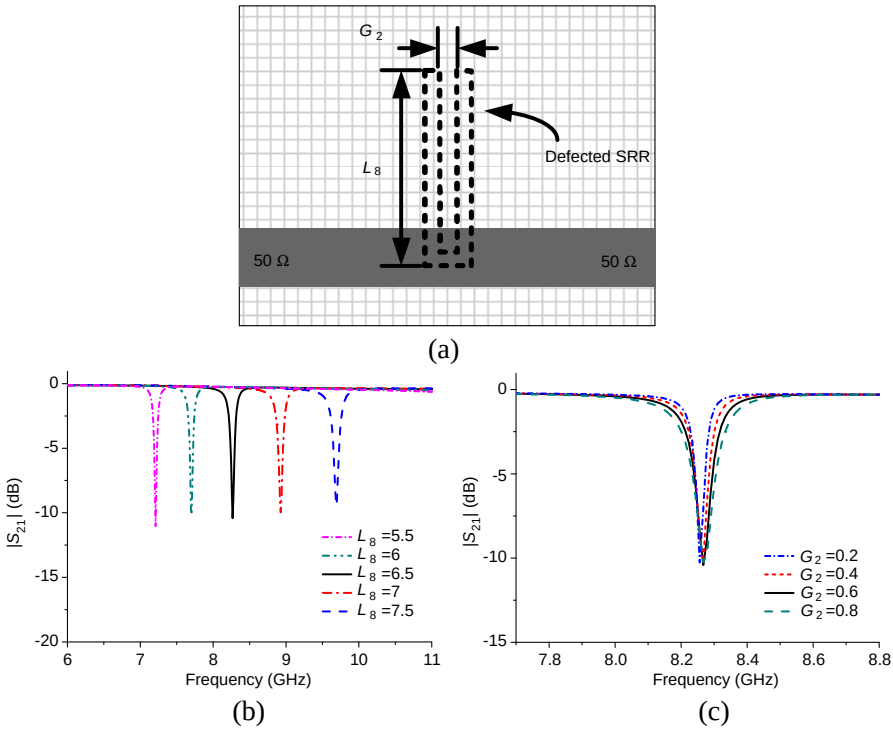


**Figure 7.** (a) Split-ring resonators. (b) Simulated result of $|S_{21}|$ with $G_2 = 0.3\,\text{mm}$ and variable $L_8$. (c) Simulated result of $|S_{21}|$ with $L_8 = 6.5\,\text{mm}$ and variable $G_2$.

UWB passband, defined as:

$$\text{S.F.} = \frac{\Delta f_{3\,\text{dB}}}{\Delta f_{30\,\text{dB}}} \tag{10}$$

where $\Delta f_{3\,\text{dB}}$, $\Delta f_{30\,\text{dB}}$ represent for 3 dB bandwidth and 30 dB bandwidth of passband, respectively. Table 1 is the comparison of the proposed UWB filter with the reported ones, where $\lambda_0$ is the free space wavelength of the operating frequency at the center of the passband. As it can be seen, the proposed UWB BPF has the advantage of sharp selectivity and compact size. As a result, it is quite useful in future wireless communication system.

Figure 8 is the photograph of the fabricated filter. The substrate used is with a relative dielectric constant of 2.65 and a thickness of 1 mm. The dimensions optimized by IE3D are $L_1 = 8.6$, $L_2 = 8.7$, $L_3 = 3.8$, $L_4 = 6.3$, $L_5 = 2.4$, $L_6 = 8.7$, $L_7 = 6$, $L_8 = 6.4$, $W_1 = 2.1$, $W_2 = 0.6$, $W_3 = 0.5$, $W_4 = 3.5$, $W_5 = 0.7$, $W_6 = 3.7$, $G_1 = 0.2$,

**Table 1.** Comparison with the reported UWB BPFs.

| Ref. | Return Loss (dB) | 3 dB FBW | S.F. | Notched Band (GHz) | Size ($\lambda_0 \times \lambda_0$) | Upper stopband (GHz) |
|---|---|---|---|---|---|---|
| [7] | 10 | 113% | 0.625 | no | 0.37×0.04 | no |
| [8] | 9.8 | 109% | 0.796 | Yes, (@5.8) | 0.37×0.08 | Yes, (13.0–18.0) |
| [9] | 5.9 | 112% | 0.793 | no | 0.14 × 0.13 | Yes, (12.0–26.0) |
| [10] | 13.1 | 109% | 0.815 | no | 0.36 × 0.24 | Yes, (12.5-18.3) |
| [11] | 14.3 | 114% | 0.743 | no | 0.48 × 0.09 | Yes, (11.1–17.1) |
| [14] | 8.3 | 110% | 0.904 | no | 0.49 × 0.93 | no |
| [16] | 10.1 | 103% | 0.852 | Yes, (@5.4) | 0.6 × 0.27 | Yes, (11.6–16.1) |
| Proposed Filter | 10.3 | 106% | 0.911 | Yes, (@8.6) | 0.51 × 0.32 | Yes, (10.7–16.3) |

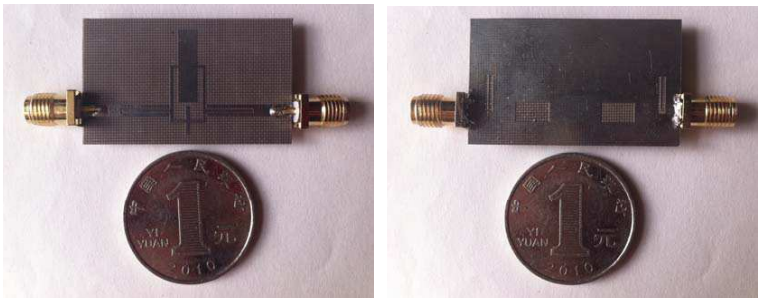

(a) (b)

**Figure 8.** Photograph of the fabricated UWB filter. (a) Top view. (b) Bottom view.

$G_2 = 0.3$ (all in millimeters). Figure 9 is the simulated and measured results of proposed UWB BPF, and good agreement between simulated and measured results is observed. As shown in Figure 9(a), the 3 dB passband covers the range of 3.2–10.4 GHz, and it has a fractional bandwidth of 106%. A single notched band is measured at 8.6 GHz

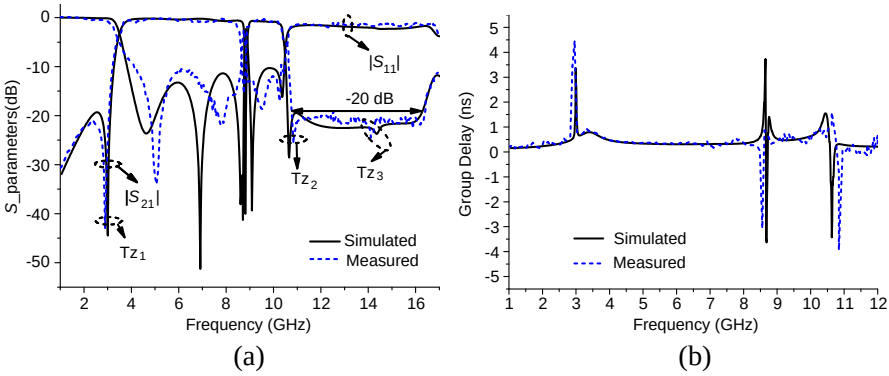


**Figure 9.** Simulated and measured frequency responses of fabricated UWB BPF. (a) $S$-magnitudes. (b) Group delay.

with 11.2 dB insertion loss and 3 dB notch bandwidth of 1.4%. The measured return loss is better than 10.3 dB in the UWB passband except the notched band. The harmonic responses over the frequency range from 10.7 to 16.3 GHz are suppressed for more than 20 dB. In addition, the group delay of this UWB bandpass filter can be calculated by

$$\tau = -\frac{\partial \angle S_{21}}{\partial \omega} \tag{11}$$

where $\angle S_{21}$ is the insertion-loss phase and $\omega$ the frequency in radians per second. Figure 9(b) shows the group delay of the filter. the group delay in most of the passband is between 0.25–0.70 ns. Serious variation in group delay is primarily due to the sharp rejection skirt around the notched band and the finite transmission zeros.

Owing to the two transmission zeros in the lower and upper cutoff frequencies, sharp selectivity is achieved. In addition, discrepancy between measured and simulated results may be caused by approximate fabrication precision wide-band calibration and parasitic effects of the SMA connector.

## 4. CONCLUSION

In this paper, a compact UWB BPF with improved sharp skirt and emerged notch-band has been proposed and designed. The MSLRR is constructed by loading four open stubs in a ring resonator, and five modes, including two odd modes and three even modes within the desired band are combined to realize UWB passband. Two transmission zeros on both sides of the pass-band result in a high

frequency selectivity of the filter. Meanwhile, a wide upper-stopband with the insertion loss higher than 20 dB in range of 10.7 to 16.3 GHz is achieved. A notched band is introduced by embedding two SRRs in the input/output lines. Excellent agreement between the predicted and measured results is obtained. Owing to its simple topology, planar implementation and high performance, it is very attractive in the practical applications.

## ACKNOWLEDGMENT

This work was supported by the National Natural Science Foundation of China (NSFC) under project No. 61271017.

## REFERENCES

1. "Revision of Part 15 of the Commission's rules regarding ultra-wideband transmission system," Federal Communications Commission, ET-Docket 98-153, 2002.
2. Lin, Y. S., W. C. Ku, C. H. Wang, and C. H. Chen, "Wideband coplanar-waveguide bandpass filters with good stopband rejection," *IEEE Microw. Wireless Compon. Lett.*, Vol. 4, No. 9, 422–424, Sep. 2004.
3. Shobeyri, M. and M. H. Vadjed-Samiei, "Compact ultra-wideband bandpass filter with defected ground structure," *Progress In Electromagnetics Research Letters*, Vol. 4, 25–31, 2008.
4. Mirzaee, M., "A novel small ultra-wideband bandpass filter including narrow notched band utilizing folded-T-shaped stepped impedance resonator (SIR)," *Progress In Electromagnetics Research C*, Vol. 22, 85–96, 2011
5. Gao, S. S., X. S. Yang, J. P. Wang, S. Q. Xiao, and B. Z. Wang, "Compact ultra-wideband (UWB) bandpass filter using modified stepped impedance resonator," *Journal of Electromagnetic Waves and Applications*, Vol. 22, No. 4, 541–548, 2008.
6. Lee, C. H., I.-C. Wang, and L. Y. Chen, "MMR-based band-notched UWB bandpass filter design," *Journal of Electromagnetic Waves and Applications*, Vol. 22, Nos. 17–18, 2407–2415, 2008.
7. Gao, M.-J., L.-S. Wu, and J.-F. Mao, "Compact notched ultra-wideband bandpass filter with improved out-of-band performance using quasi-electromagnetic bandgap structure," *Progress In Electromagnetics Research*, Vol. 125, 137–150, 2012.
8. Ghazali, A.-N., and S. Pal, "Analysis of a small UWB filter

with notch and improved stopband," *Progress In Electromagnetics Research Letters*, Vol. 34, 147–156, 2012.

9. Zhu, L., S. Sun, and W. Menzel, "Ultra-wideband (UWB) bandpass filters using multiple-mode resonator," *IEEE Microw. Wireless Compon. Lett.*, Vol. 15, No. 11, 796–798, Nov. 2005.
10. Chen, L., F. Wei, X.-W. Shi, and C.-J. Gao, "An ultra-wideband bandpass filter with a notched-band and wide stopband using dumbbell stubs," *Progress In Electromagnetics Research Letters*, Vol. 17, 47–53, 2010.
11. Tian, X.-K. and Q.-X. Chu, "A compact UWB bandpass filter with improved out-of-band performance using modified coupling structure," *Progress In Electromagnetics Research Letters*, Vol. 22, 191–197, 2011.
12. Deng, H.-W., Y.-J. Zhao, L. Zhang, X.-S. Zhang, and W. Zhao, "Novel UWB BPF using quintuple-mode stub-loaded resonator," *Progress In Electromagnetics Research Letters*, Vol. 14, 181–187, 2010.
13. Shen, Y.-Z. and C.-L. Law, "5.8-GHz suppressed UWB bandpass filter employing modified CRLH-TL of two and three unit cells," *Progress In Electromagnetics Research Letters*, Vol. 29, 107–113, 2012.
14. Kim, C.-H. and K. Chang, "Ultra-wideband (UWB) ring resonator bandpass filter with a notched band," *IEEE Microw. Wireless Compon. Lett.*, Vol. 21, No. 4, 206–208, Apr. 2011.
15. Shi, S., W.-W. Choi, W. Che, K.-W. Tam, and Q. Xue, "Ultra-wideband differential bandpass filter with narrow notched band and improved common-mode suppression by DGS," *IEEE Microw. Wireless Compon. Lett.*, Vol. 2, No. 4, 185–187, Apr. 2012.
16. Naghshvarian-Jahromi, M. and M. Tayarini, "Defected ground structure band-stop filter by semicomplementary split ring resonator," *IET Microw. Antennas Propag.*, Vol. 5, No. 11, 1386–1391, Aug. 2011.
17. Wei, F., Q.-Y. Wu, X.-W. Shi, and L. Chen, "Compact UWB bandpass filter with dual notched bands based on SCRLH resonator," *IEEE Microw. Wireless Compon. Lett.*, Vol. 21, No. 1, 28–30, Jan. 2011.
18. Hao, Z.-C., J.-S. Hong, S.-K. Alotaibi, J.-P. parry, and D.-P. Hand, "Ultra-wideband bandpass filter with multiple notch-bands on multilayer liquid crystal polymer substrate," *IET Microw. Antennas Propag.*, Vol. 3, No. 5 749–756, Aug. 2009.
19. Nosrati, M. and M. Daneshmand, "Compact microstrip UWB

double/single notch-band BPF based on wave's cancellation theory," *IET Microw. Antennas Propag.*, Vol. 6, No. 7, 862–868, Jun. 2012.

20. Hsiao, P.-Y. and R.-M. Weng, "Compact tri-layer ultra-wideband band-pass filter with dual notch bands," *Progress In Electromagnetics Research*, Vol. 106, 49–60, 2010.
21. Sarkar, P., M. Pal, R. Ghatak, and D.-R. Poddar, "Miniaturized UWB bandpass filter with dual notch bands and wide upper stopband," *Progress In Electromagnetics Research Letters*, Vol. 38, 161–170, 2013.
22. Kamma, A., S.-R. Gupta, G.-S. Reddy, and J. Mukherjee, "Multi-band notch UWB band pass filter with novel contiguous split rings embedded in symmetrically tapered elliptic rings," *Progress In Electromagnetics Research C*, Vol. 39, 133–148, 2013.
23. Hsieh, L.-H. and K. Chang, "Compact, low insertion-loss, sharp-rejection, and wide-band microstrip bandpass filters," *IEEE Trans. Microwave Theory Tech.*, Vol. 51, No. 4, 1241–1246, Apr. 2003.
24. Sun, S. and L. Zhu, "Wideband microstrip ring resonator bandpass filters under multiple resonances," *IEEE Trans. Microwave Theory Tech.*, Vol. 55, No. 10, 2176–2182, Oct. 2007.
25. Shaman, H. and J.-S. Hong, "A novel ultra-wideband (UWB) bandpass filter (BPF) with pairs of transmission zeroes," *IEEE Microw. Wireless Compon. Lett.*, Vol. 17, No. 2, 121–123, Feb. 2007.
26. Matthaei, G. L., L. Young, and E. M. T. Jones, *Microwave Filters, Impedance-matching Networks, and Coupling Structures*, Artech House, Dedham, 1980.